A combined differential scanning calorimetry and thermogravimetry approach for the effective assessment of drug substance-excipient compatibility

Barbara Rojek[1] · Marek Wesolowski[1]

Abstract

Differential scanning calorimetry (DSC) is a tool particularly recommended for rapid compatibility screening between active pharmaceutical ingredients (APIs) and excipients, whereas thermogravimetric analysis (TGA), a complementary technique to DSC, is primarily used to assess the thermal stability of APIs and excipients. Both DSC and TGA data can be converted using multivariate statistical methods, which are profitable tools in the detection of compatibility between ingredients. Principal component analysis (PCA) enables identification of compatibility by grouping samples into two clusters in a PCA score plot: acetazolamide and mixture with its highest content, and optionally a 1:1 mixture form one cluster, excipient and mixture with its highest quantity, and optionally a 1:1 mixture the second. Any variation from the arrangement of samples in the abovementioned clusters indicates incompatibility. By using cluster analysis, compatibility can be determined by four clusters, the first consisting of API, the second of groups mixture at the ratio of 7:3 and the third of two mixtures at ratios of 3:7 and 1:1, with the excipient in the remaining fourth cluster. Generally, the combination of DSC and TGA techniques with advanced statistical methods is favorable for the qualitative assessment of compatibility in acetazolamide mixtures with excipients such as mannitol, meglumine, lactose, magnesium stearate, β-cyclodextrin, chitosan, methylcellulose, starch 1500 and PVP K-30. In addition, PXRD revealed that acetazolamide retains its crystalline form after mixing. Accordingly, incompatibilities in acetazolamide mixtures can be attributed to chemical reactions.

Keywords DSC · TGA · Advanced statistical methods · PXRD · Compatibility

Introduction

Differential scanning calorimetry (DSC) and thermogravimetric analysis (TGA) are widely used analytical methods whose employment in the study of pharmaceuticals has been constantly on the increase. Thermal methods (DSC and TGA) rely on linear heating/cooling of the tested samples and measurement of the temperatures and heats of phase transitions or mass loses occurring under these conditions. These methods make it possible to study physical processes, including melting, sublimation, dehydration, crystallization, polymorphic transformations and glass transition, as well as chemical processes such as thermal degradation [1]. One extremely important element is the utilization of thermal methods to solve issues related to pharmaceutical technology, that is, compatibility examination between active pharmaceutical ingredients (APIs) and excipients in formulated medicinal products. The results acquired allow for a concurrent selection of excipients in order to determine the pathways of degradation in the APIs [2]. Hence, to obtain effective and safe pharmaceutical preparations, the selection of excipient is extremely important [3], no less so on account of the presence of "reactive impurities" in the excipient that could contribute to API degradation [4]. As the leading analytical methods in pharmaceutical technology, DSC and TGA are applied for API-excipient compatibility and stability assessment, and quality control of drug formulations [5, 6]. DSC allows the rapid screening of possible incompatibilities in drug products by revealing changes in melting endotherms due to the shifting, disappearance of peaks or the appearance of new ones, variations in the values of enthalpy

✉ Barbara Rojek
  rojekb@gumed.edu.pl

1 Department of Analytical Chemistry, Faculty of Pharmacy, Medical University of Gdansk, Gen. J. Hallera 107, 80-416 Gdańsk, Poland

of fusion, and alterations in the decomposition pathway as compared to the separate ingredients [7]. However, inconsiderable changes in the peak parameters, i.e., width, height and shape, can be attributed to probable differences in mixture composition. It should be noted that when the thermal properties of the mixtures, including melting point, heat of fusion and others, are the sum of the individual ingredients, then ingredients are absolutely compatible [2]. In turn, TGA is a complementary method to DSC due to its limitations in the assessment of compatibility. Interpretation of TGA is based on a comparison of thermal curve of API alone with that of physical mixtures containing API and excipients. The changes observed in the TGA curve of the mixtures in relation to the curve of API provide information on the stability of the API in the presence of excipients and, consequently, about its compatibility with these excipients [8].

Despite the fact that DSC is the primary method recommended for rapid compatibility screening, conclusions drawn solely from DSC may sometimes be unclear and require careful interpretation of the results [2]. Likewise, TGA used separately can sometimes lead to questionable conclusions. Samples analyzed with DSC or TGA are typically heated to about 300 °C, while drug formulations are stored at ambient conditions. However, the incompatibilities found at higher temperatures sometimes do not occur under storage conditions [2, 9, 10]. The kinetics of reaction increases with a rise in temperature, which may change the physicochemical properties of ingredients [10]. On the other hand, the ambiguous interpretation of the data acquired from thermal methods demands the use of assistive techniques [2, 9].

Since the interpretation of thermal analysis data does not always prove satisfactory, it may be beneficial to include advanced statistical methods. Two of these, principal component (PCA) and cluster (CA) analyses, can be used for this purpose. PCA as a dimension-reduction tool is applicable to data reduction leading to the emergence of a new set of orthogonal variables, i.e., principal components (PCs) used to describe variability in the data [11]. In contrast to PCA, CA evaluates the trend of sample clustering using an agglomeration schedule to aggregate samples according to the distance between sample pairs and the difference in the linking algorithms by which samples or clusters are merged [11, 12]. As the thermal methods provide various types of thermodynamic information, multivariate statistical methods in the interpretation of these data are particularly beneficial, especially in the case of questionable interpretation of DSC or TGA alone.

Therefore, the aim of the study was to develop a method for detecting incompatibility by a combination of DSC and TGA and an additional combination with advanced statistical methods. This combination makes it possible to improve our understanding of the thermal behavior of both ingredients, alone and in mixtures. For this purpose, model acetazolamide binary mixtures with selected excipients, such as mannitol, meglumine, lactose, magnesium stearate, β-cyclodextrin, chitosan, methylcellulose, starch 1500 and polyvinylpyrrolidone (PVP K-30), were analyzed. PCA and CA were applied to acquire additional information, not directly available from the DSC and TGA curves.

Acetazolamide (Fig. 1) is a sulfonamide carbonic anhydrase inhibitor, which it has been in use as an API since the 1950s for the treatment of various conditions, e.g., sleep apnea, altitude sickness, glaucoma, or epilepsy, but its application is often restricted due to side effects, which may be dose related [13].

Materials and methods

Materials

Acetazolamide marketed under the trade name Diamox (m.p. 258–259 °C, purity ≥ 99%) was obtained from Polfa (Warsaw, Poland), meglumine (m.p. 126–131 °C, purity ≥ 99%), β-cyclodextrin (m.p. 290–300 °C, purity ≥ 99%), chitosan shrimp shells, low viscous (glass transition at 203 °C, purity ≥ 95%) and polyvinylpyrrolidone (PVP K-30) (decomposition > 150 °C, purum) from Fluka (Siegen, Germany), lactose (m.p. 232 °C, purity Ph. Eur.) from BUFA B.V. (Uitgeest, Netherlands), magnesium stearate (m.p. 126–130 °C, purity Ph. Eur.) from Faci (Carasco Genoa, Italy), methylcellulose (decomposition 280–300 °C, purity Ph. Eur.) from the Shin'etsu Chemical Co. (Tokyo, Japan), mannitol (166–168 °C, purity Ph. Eur.) from POCh (Gliwice, Poland) and starch 1500 (decomposition > 220 °C, purity Ph. Eur.) from Colorcon (Harleysville, PA, USA).

Sample preparation

Binary mixtures of acetazolamide with β-cyclodextrin, methylcellulose, starch 1500 and PVP K-30 were composed at the mass ratios, with mixtures with mannitol, meglumine, lactose, magnesium stearate and chitosan being mixed at the molar ratios. After weighing on an analytical balance XA 105 (Mettler Toledo, Switzerland), acetazolamide and excipients at ratios of 7:3, 1:1 and 3:7 were poured into an agate mortar and homogenized with a plastic spatula over 5 min.
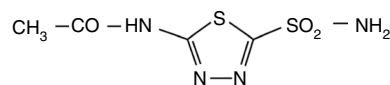

Fig. 1 Molecular structure of acetazolamide

Thermal analysis

A DSC 822e device (Mettler Toledo, Schwerzenbach, Switzerland) controlled by STARe 9.10 software and equipped with Dewar vessel was used for the analysis of the samples under study. The 4–5 mg samples were weighed into 40 μL aluminum pans and the reference sample into an empty pan. Additionally, all pans were hermetically sealed with a pierced lid. Measurements were taken from 25 to 300 °C, at a heating rate of 10 °C min^{-1}. During the heating–cooling–reheating program, acetazolamide was heated at a rate of 10 °C min^{-1}, kept at 300 °C for 2 min, then cooled from 300 to −25 °C at a rate of 10 °C min^{-1}, kept at −25 °C for 2 min, and finally reheated up to 300 °C at a rate of 10 °C min^{-1}. All measurements were carried out under nitrogen (purity 99.9997%) with a flux rate of 70 mL min^{-1}. The values of onset and peak temperatures (T_{onset} and T_{peak}) and the heats of fusion (ΔH) were acquired from the DSC curves using STARe 9.10 software.

Indium and zinc standards (Mettler Toledo, Schwerzenbach, Switzerland) were used for the calibration of the DSC cell. The data obtained for the standards (onset temperatures and heat flows), 156.6 °C and 28.45 J g^{-1} for indium, and 419.6 °C and 107.5 J g^{-1} for zinc, respectively, were consistent with those in the literature [14].

TGA sample analysis was performed using an OD-103 Derivatograph (MOM, Budapest, Hungary). About 200 mg of the samples was heated in four flat-bottomed platinum crucibles at a rate of 5 °C min^{-1} up to 700 °C in air atmosphere against alumina as reference substance. From TGA and DTG curves, the values of temperature ranges of mass losses (ΔT), DTG peaks temperatures (T_{peak}) and mass losses (Δm) for thermal degradation were obtained. Calcium oxalate dihydrate was used to calibrate the Derivatograph.

Powder X-ray diffraction (PXRD)

PXRD analyses were performed on a D2 Phaser diffractometer (Bruker, Karlsruhe, Germany) using DIRRRAC.SUITE software to record the diffraction patterns. Measurements were taken with a CuKα tube ($k = 0.154060$ nm) under ambient condition, in the range of 7°–55° at 30 kV and 10 mA, at a digitalization speed of 0.02° and at angle intervals of 2θ and an exposure time of 0.10 s.

Advanced statistical analysis

Two advanced statistical methods (PCA and CA) were used for the evaluation of the DSC and TGA datasets. The decision was taken to perform statistical calculations on combined DSC and TGA data. A total set of nine matrices were constructed for PCA and CA calculations, i.e., separate matrix for each individual excipient (mannitol, meglumine, lactose, magnesium stearate, β-cyclodextrin, chitosan, methylcellulose, starch 1500 and PVP K-30). Each matrix has a dimension of 5 × 18, where 5 specifies the number of objects (rows) and 18 the number of variables (columns). The rows of the matrix consisted of acetazolamide, excipient and their mixtures at the ratios 7:3, 1:1 and 3:7, while columns contained the values of T_{onset}, T_{peak}, ΔH acquired from the DSC curves (Tables 1–2), and ΔT, T_{peak}, Δm obtained from the TGA and DTG curves (Tables 3–4). The data acquired from DSC and TGA/DTG curves were used for multivariate calculations without further preprocessing.

The statistical model was created using Statistica StatSoft Inc. ver. 13.3 (Tulsa, OK, USA). Ward's method (agglomerative hierarchical clustering) with Euclidian distance was used to build the CA dendrogram and Sneath's index criterion to find the number of significant clusters at 2/3 of the maximum distance. PCA calculations were executed with an algorithm, disregarding the rotation of factors and correlation matrices. Five principal components were obtained for each matrix. Because the first two principal components explained together more than 81% of the total variability, the findings of the PCA calculations were presented in the form of two-dimensional score scatter plot. The third, fourth and fifth principal components were not used because they explained too little of the total variability.

Results and discussion

DSC constitutes the dominant instrumental technique that has increasingly being used for the rapid screening of API-excipient compatibility. However, the incompatibilities identified by DSC should be affirmed by other tools in the further stages of any study [15, 16].

Incompatibility is detected by comparing the DSC curves of mixtures with those of individual ingredients [15, 17]. Through DSC, information is acquired about the peak temperature, heat, shifts of endothermic or exothermic effects, and the appearance or disappearance of any new ones [5, 18]. The visual alterations on the DSC curve of binary mixture and changes in the value of thermodynamic parameters compared to those for the ingredients alone indicate incompatibilities between ingredients. In contrast, the DSC curve of a mixture is the sum of the thermal effects of all its constituent ingredients, if compatible [2]. TGA, in turn, shows only the percentage mass loss as a function of temperature, which is a limitation in compatibility studies [8].

Thermal characterization of acetazolamide

The DSC curve of acetazolamide (Fig. 3, the first heating) displays a single endothermic peak attributed to melting with decomposition at 260.88 °C (fusion heat −164.64 J g^{-1}),

Table 1 DSC data for acetazolamide and its mixtures with analyzed excipients

Sample	API/ excipient ratio	Thermal event 1			Thermal event 2			Thermal event 3		
		T_{onset}/°C	T_{peak}/°C	ΔH/J g^{-1}	T_{onset}/°C	T_{peak}/°C	ΔH/J g^{-1}	T_{onset}/°C	T_{peak}/°C	ΔH/J g^{-1}
Acetazolamide	–	–	–	–	258.43	261.73	−213.72	266.45	271.49	101.55
Acetazolamid: mannitol	7:3	163.60	166.52	−73.44	233.00	243.13	−143.46	249.16	254.95	98.15
	1:1	164.04	166.48	−134.80	214.76	228.50	−84.71	243.50	248.88	39.08
	3:7	151.25	166.86	−187.27	208.76	220.67	−31.55	225.70	240.34	44.74
Acetazolamide: meglumine	7:3	106.78	115.27	−55.40	189.00	196.63	−104.61	221.15	236.75	73.26
	1:1	102.24	114.42	−99.49	160.06	189.85	27.90	217.48	227.45	77.60
	3:7	112.76	119.87	−141.41	195.23	200.11	181.40	–	–	–
Acetazolamide: lactose	7:3	142.84	146.69	−57.42	201.69	213.16	−167.22	231.00	238.47	96.57
	1:1	144.04	146.56	−87.67	203.69	210.60	−196.13	222.12	226.74	87.34
	3:7	143.07	146.13	−106.41	208.09	213.56	−199.96	228.35	233.46	59.32
Acetazolamide: magnesium stearate	7:3	93.02	104.90	−158.86	250.64	255.21	−72.80	258.45	262.99	11.58
	1:1	93.71	106.32	−195.99	227.91	232.37	−22.00	–	–	–
	3:7	94.06	106.60	−265.55	193.90	212.05	−15.42	250.94	256.28	11.37
Acetazolamide: β-cyclodextrin	7:3	82.26	108.23	−59.50	256.81	260.50	−150.41	265.63	271.59	163.89
	1:1	163.23	164.24	−118.04	256.60	259.11	−79.87	273.82	276.20	64.26
	3:7	98.18	125.55	−225.42	254.78	260.24	−65.75	277.30	278.68	35.81
Acetazolamide: chitosan	7:3	45.08	87.62	−47.71	246.31	255.58	−189.11	262.33	268.00	116.08
	1:1	47.70	107.56	−144.12	238.19	251.43	−134.26	261.74	268.14	83.52
	3:7	27.37	84.22	−174.16	228.37	253.86	−116.48	–	–	–
Acetazolamide: methylcellulose	7:3	45.24	68.64	−6.78	257.03	262.19	−172.70	268.74	273.69	48.47
	1:1	44.59	83.63	−38.70	254.00	259.01	−94.44	–	–	–
	3:7	42.62	88.94	−73.28	256.65	262.04	−49.00	268.90	274.01	4.97
Acetazolamide: starch 1500	7:3	44.13	94.45	−56.65	250.43	253.06	−126.74	259.93	266.34	94.19
	1:1	71.70	116.19	−60.47	261.70	263.72	−129.54	268.62	270.59	20.34
	3:7	29.59	90.41	−180.25	238.94	262.40	−101.19	270.12	271.50	66.54
Acetazolamide: PVP K-30	7:3	110.06	118.15	−59.18	183.52	199.86	−160.07	231.28	239.42	85.50
	1:1	56.01	112.18	−167.34	212.47	255.60	−88.34	258.96	274.46	66.50
	3:7	26.79	102.37	−236.03	249.70	260.70	−43.22	269.30	287.97	13.81

Table 2 DSC data for excipients

Excipient	Thermal events		
	T_{onset}/°C	T_{peak}/°C	ΔH/J^{-1}
Mannitol	165.52	167.54	−282.3
Meglumine	127.97	128.88	−310.62
Lactose	141.93	143.68	−135.69
	213	218.91	−305.69
		239.59	
Magnesium stearate	93.27	70.97	−305.73
		106.95	
		120.05	
β-cyclodextrin	27.02	116.08	−372.12
Chitosan	27.99	117.71	−229.95
Methylcellulose	29.2	77.61	−72.56
Starch 1500	26.59	100.9	−213.38
PVP K-30	52.52	109.76	−116.42

which is consistent with the literature data [19, 20]. The second exothermic peak can be found at 272.42 °C with an enthalpy value 69.07 J g^{-1} (Table 1).

Acetazolamide decomposes immediately upon melting, but its decomposition products are not described in the literature. This substance is broken down in three subsequent stages, as reported in our previous work [21]. As can be seen from the TGA curve, the first stage takes place in the range of 220–264 °C with 62% mass loss, which is probably related to formation of sulfur dicyanide by disconnection of the sulfonamide group and acetamide. The second stage occurs between 264 and 296 °C with ~17% mass loss due to evaporation of sulfur dicyanide, and the final, third stage over the range 296–450 °C with combustion of charred residue (Table 3). Thus, a proposed mechanism of acetazolamide decomposition is presented in Fig. 2.

The second heating curve of acetazolamide shown in Fig. 3 reveals the glass transition of the new amorphous

Table 3 TGA data for acetazolamide and its mixtures with analyzed excipients

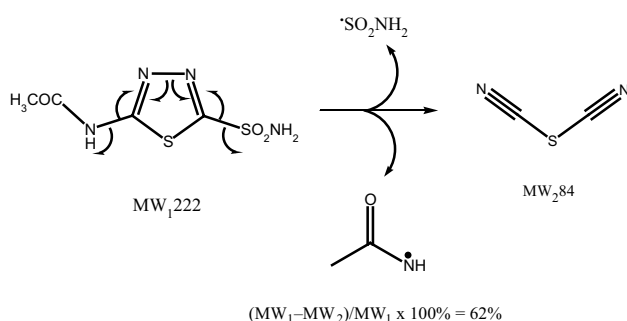| Sample	API/ excipient ratio	Decomposition								
		Stage 1			Stage 2			Stage 3		
		ΔT/°C	T_{peak}/°C	Δm/%	ΔT/°C	T_{peak}/°C	Δm/%	ΔT/°C	T_{peak}/°C	Δm/%
Acetazolamide	–	–	–	–	170–260	200	62	260–350	300	17
								350–500	400	21
Acetazolamide: mannitol	07:03	–	–	–	145–280	200, 210	73	280–560	510	27
	01:01	–	–	–	105–270	185, 195	76	270–550	440	24
	03:07	–	–	–	110–290	180, 215	80	290–530	480	20
Acetazolamide: meglumine	07:03	–	–	–	100–320	180, 220	72	320–610	510	28
	01:01	–	–	–	100–320	170, 225	69	320–545	470	31
	03:07	–	–	–	100–320	170, 230	69	320–540	470	31
Acetazolamide: lactose	07:03	80–140	100	2	140–310	170	66	310–550	470	32
	01:01	80–140	105	3	140–310	170	64	310–570	470	33
	03:07	80–140	100	4	140–320	175	59	320–570	480	37
Acetazolamide: magnesium stearate	07:03	40–120	50	6	120–320	200, 270	56	320–560	500	33
										residue 5.0
	01:01	30–140	70	2	140–250	200	30	420–560	460	17
					250–420	300	46			residue 5.0
	03:07	20–110	60	4	110–280	200, 250	20	390–530	440	20
					280–390	320, 355	46			residue 10.0
Acetazolamide: β-cyclodextrin	07:03	20–130	60	4	130–330	210, 220	68	330–580	430	28
	01:01	20–140	60	9	140–340	205, 220	63	340–550	430	28
	03:07	20–150	60	9	150–330	210, 230	59	330–570	430	22
Acetazolamide: chitosan	07:03	20–100	50	3	140–290	200	59	290–590	500	38
	01:01	20–100	50	4	120–290	205	55	290–550	475	41
	03:07	20–110	50	6	110–300	205, 235	49	300–510	380	45
Acetazolamide: methylcellulose	07:03	20–120	30	2	120–345	200	72	345–590	520	26
	01:01	20–130	35	2	130–350	205	72	350–570	500	26
	03:07	20–140	40	4	140–345	205	71	345–580	480	25
Acetazolamide: starch 1500	07:03	20–110	45	3	110–310	190	68	310–560	480	29
	01:01	20–130	50	5	130–330	195, 210	65	330–590	460	30
	03:07	20–130	50	6	130–330	200, 220	61	330–560	460	33
Acetazolamide: PVP K-30	07:03	20–140	45	3	140–330	205, 230	59	330–580	480	38
	01:01	20–120	40	5	120–305	200, 230	47	385–580	480	32
					305–385	350	16			
	03:07	20–140	50	7	140–290	200	34	380–580	480	33
					290–380	340	26			

product formed during the decomposition of the melted sample while the first heating. The presence of the amorphous product was confirmed by PXRD analysis performed for acetazolamide at successive temperatures until the API melting. As shown in Fig. 4, the last diffraction pattern recorded after cooling the sample to room temperature confirms the formation of an amorphous product.

Acetazolamide compatibility studies

As acetazolamide decomposes upon melting, the heating DSC program can only be used for compatibility confirmation. Figures 5 and 6 illustrate the DSC, TGA and derivative thermogravimetric (DTG) curves of acetazolamide, chitosan and their binary mixtures. The DSC curve of

Table 4 TGA data for excipients

Excipient	Decomposition								
	Stage 1			Stage 2			Stage 3		
	$\Delta T/°C$	$T_{peak}/°C$	$\Delta m/\%$	$\Delta T/°C$	$T_{peak}/°C$	$\Delta m/\%$	$\Delta T/°C$	$T_{peak}/°C$	$\Delta m/\%$
Mannitol	–	–	–	150–320	260	96	320–480	370	4
Meglumine	–	–	–	130–330	210	75	330–510	420	25
Lactose	85–140	110	4.5	140–200	180	10	320–490	430	30.5
				200–320	230	54			
Magnesium stearate	40–130	70	4	130–260	205	17	365–680	395	10
				260–365	320	62			
β-cyclodextrin	40–120	70	13	185–325	265	65	325–525	430	22
Chitosan	30–140	60	8	140–315	240	58	315–470	430	34
Methylcellulose	30–80	50	2	155–285	260	78	285–690	405	20
Starch 1500	30–155	60	10	155–230	200	23	290–510	445	49
				230–290	260	18			
PVP K-30	30–100	50	6	160–310	275	25	380–570	485	44
				310–380	335	25,0			

$$(MW_1 - MW_2)/MW_1 \times 100\% = 62\%$$

Fig. 2 Suggested pathway of degradation of acetazolamide based on TGA

chitosan (Fig. 5e, Table 2) exhibits two broader endothermic peaks at 117.7 °C and 275.9 °C assigned to dehydration with the heat of -229.9 J g^{-1} and glass transition, respectively. These are followed by the decomposition of the polymeric chain and the evaporation of volatiles. These thermal events are reflected on the TGA curve by mass loss of 8.0% in the range of 30–140 °C and 58.0% in the range of 140–315 °C, respectively (Table 4). The pyrolysis of polysaccharide structure starts with an accidental split in the glycoside bonds, which produces further decomposition as well as a series of lower fatty acids, as well as acetic and butyric acids [22].

As regards the acetazolamide-chitosan mixtures (Fig. 5b–d), all characteristic thermal events for both ingredients were observed on the DSC curves. Areas of peaks are proportional to the content of ingredients in mixture. The TGA curves also showed characteristic thermal phenomena for both ingredients with mass loss depending on the content of ingredients in these mixtures (Table 3).
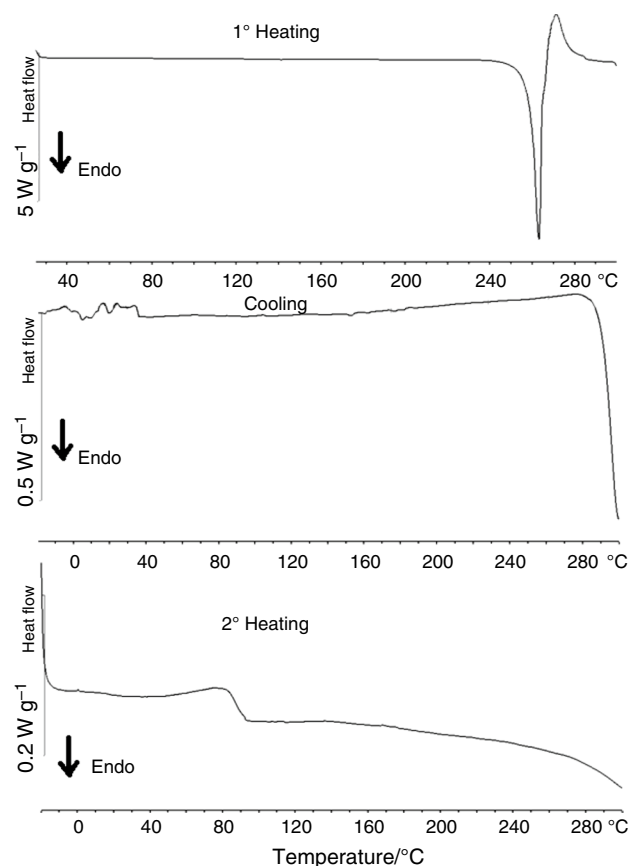

Fig. 3 DSC (1 heating–cooling–2°heating) curves of acetazolamide

Figure 6e presents a sharp endothermic DSC peak at 167.5 °C due to the melting of mannitol (Table 2, heat of fusion–282.3 J g^{-1}). The TGA curve shows a 96.0% mass
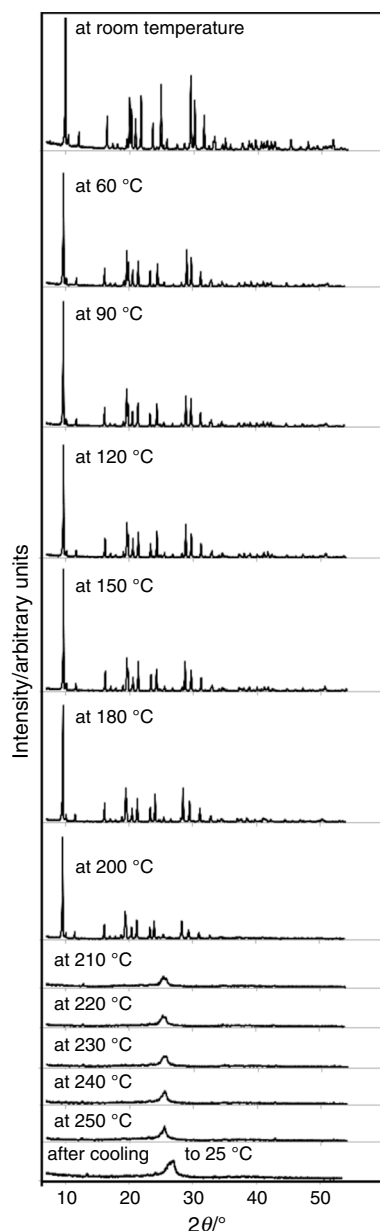
Fig. 4 PXRD patterns for acetazolamide at room temperature, at 60, 90, 120, 150, 180, 200, 210, 220, 230, 240 and 250 °C and after cooling to 25 °C

loss in the range of 150–320 °C assigned to evaporation of melted mannitol (Table 4, second stage), with combustion of carbonized residue visible at higher temperatures in the third stage. In the case of acetazolamide mixtures with mannitol (Fig. 6b–d), the characteristic DSC peaks of acetazolamide shift to lower temperatures and are widened and blurred. Gradual decreases in acetazolamide content in the mixtures results in peak expansion and shift by approx. 20 °C. The melting peak of mannitol remains, only slightly widened as the mannitol content in the mixtures increased. The course of the TGA curves for mixtures (Fig. 6b–d, Tables 3–4) differs

from that of ingredients alone. This results in temperature ranges of the thermal processes and the values of mass loss for the mixtures which differ from those for ingredients. In general terms, if no obvious incompatibility is identified in the mixture by DSC, there is no need to use supplementary tools, which are usually complex and time-consuming or often difficult to implement. Nevertheless, if characteristic peaks for ingredients disappear or new peaks appear or the temperature values of DSC events for mixtures are shifted above 5 °C to lower or, more rarely, to higher temperatures, this implies thermally promoted incompatibility. In this case, confirmatory tools such as FTIR, PXRD and others are required [6]. Moreover, advanced statistical methods can be used as supporting methods for the interpretation of ambiguous thermal data.

PXRD of acetazolamide and its mixtures with excipients (Figs. 7, 8, 9) showed that excipients did not affect the crystallinity of acetazolamide immediately after physical mixing and at room temperature, but only the intensity of its characteristic diffraction lines decreased depending on its content in the mixture. This means that there is no crystalline–amorphous conversion of acetazolamide in the presence of excipients. Hence, it is likely that the incompatibilities of acetazolamide with excipients are due to chemical reactions.

Multivariate analysis of thermal data

PCA reduces a sizeable thermal dataset to components which are simplified and orthogonal in form, ultimately classifying samples by locating patterns in the relationships between variables, thus yielding a classification of the objects [11]. The variances of the data calculated by PCA are shown in Fig. 10. This figure only shows the values for the first three principal components (PCs) due to a significant decrease in the percentage of data variance explained in the next PCs. The first principal component (PC1) alone explains over 63% of the total variability, except for the matrix of acetazolamide with methylcellulose at about 54%. Since the first two PCs (PC1 and PC2) together constitute more than 81% of total data variation, the results of PCA calculations are presented in the form of a two-dimensional plot. Based on the location of the samples on this plot, compatibility or incompatibility can be clearly indicated.

Two clusters created as a result of sample grouping can be distinguished. As regards compatibility, the first cluster holds acetazolamide and mixture with its highest content and optionally a 1:1 mixture. The excipient and mixture with the highest excipient concentration can be found in the second cluster, a 1:1 mixture again being possible. In the case of incompatibility, the distribution of samples in the clusters is unpredictable, as demonstrated in Fig. 11a, where they are cumulated in two clusters. The first, found in the negative part of the *x*-axis, includes acetazolamide and its mixture at

Fig. 5 DSC, TGA and DTG curves of **a** acetazolamide, **e** chitosan and their mixtures at the ratios: **b** 7:3, **c** 1:1 and **d** 3:7
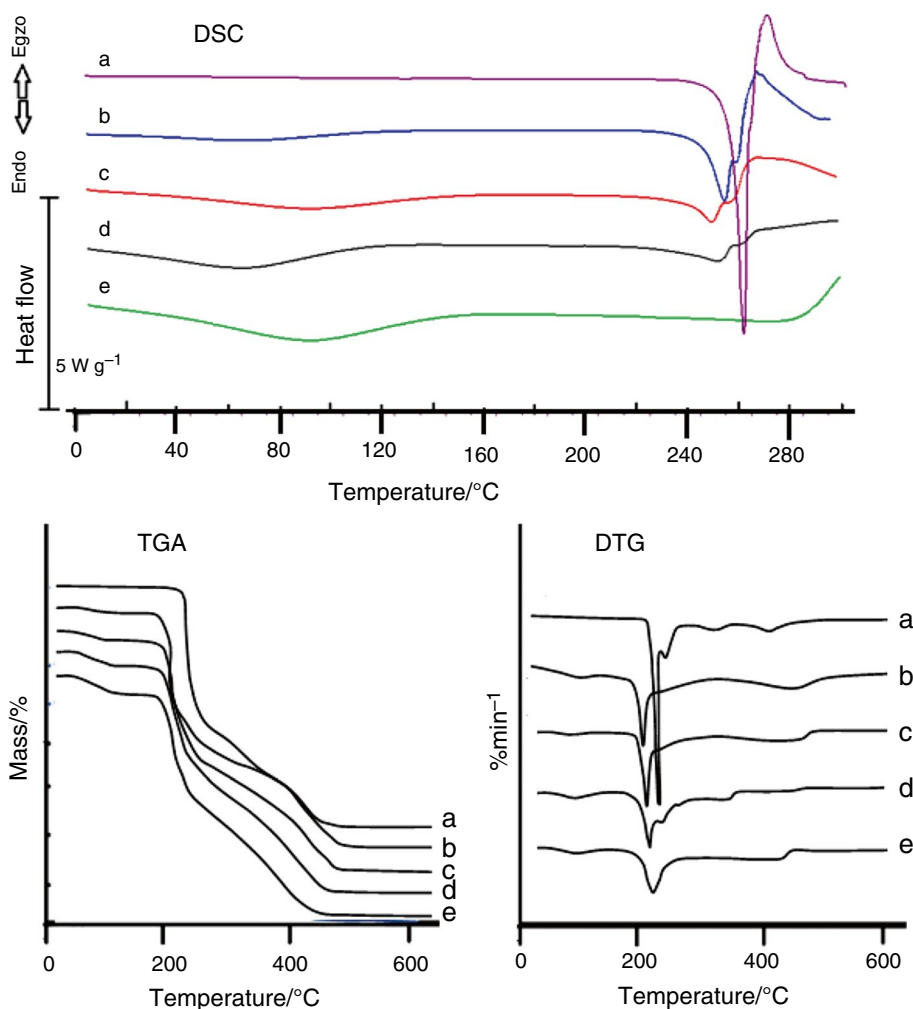
the ratio of 7:3. On the positive side of the *x*-axis, a second cluster is visible, consisting of chitosan and the remaining mixtures. Such an arrangement of samples confirms that mixture ingredients are compatible and thus can be mixed in solid dosage form technology.

In another case (Fig. 11b), the PCA plot separated two clusters, one containing acetazolamide and its mixture with mannitol at the ratio of 3:7 and the other mannitol and two mixtures at the ratio of 1:1 and 7:3. Such a distribution of samples shows the incompatibility of API and mannitol. In pharmaceutical compositions, mannitol is mainly used as a diluent in tablet formulations in an amount of 10–90% w/w. Due to the fact that this substance is not hygroscopic, it can be used with moisture-sensitive APIs. Besides, mannitol can also be used as a plasticizer, sweetener and therapeutic or tonicity agent [23].

Despite its many applications, the literature shows cases where mannitol is incompatible with APIs: with atorvastatin [24], hydroxychloroquine sulfate [25], levodopa [26], erythromycin [27] or primaquine [28]. Accordingly, various theories have been proposed to explain the incompatibility

with this excipient. One of these suggests that the amino group of API and the OH group of mannitol are linked by hydrogen bonds [24, 28], another is that the disappearance of the thermal events for API in the mixture with mannitol can be explained by the fact that the melting of this excipient occurs before API melting, which consequently leads to the dissolution of the API in the melted sugar [25]. Moreover, unlike lactose, mannitol does not undergo Maillard reactions [23]. Many examples of the incompatibility of lactose as the reducing disaccharide with APIs containing amino groups can be found in the literature. The amino sugar meglumine also causes incompatibility with glipizide, for example, but the mechanism is unknown [29].

Despite magnesium stearate being widespread as a lubricant in the pharmaceutical industry, it often contributes to the chemical instability of API [30]. Its affect on API stability is mainly due to magnesium oxide impurities, catalytic effect, alkalinity, and other chemical reactions initiated and mediated by magnesium ions [29]. Theories to explain the mechanism of chemical incompatibility have been put forward, such as that magnesium stearate causes

Fig. 6 DSC, TGA and DTG curves of **a** acetazolamide, **e** mannitol and their mixtures at the ratios: **b** 7:3, **c** 1:1 and **d** 3:7
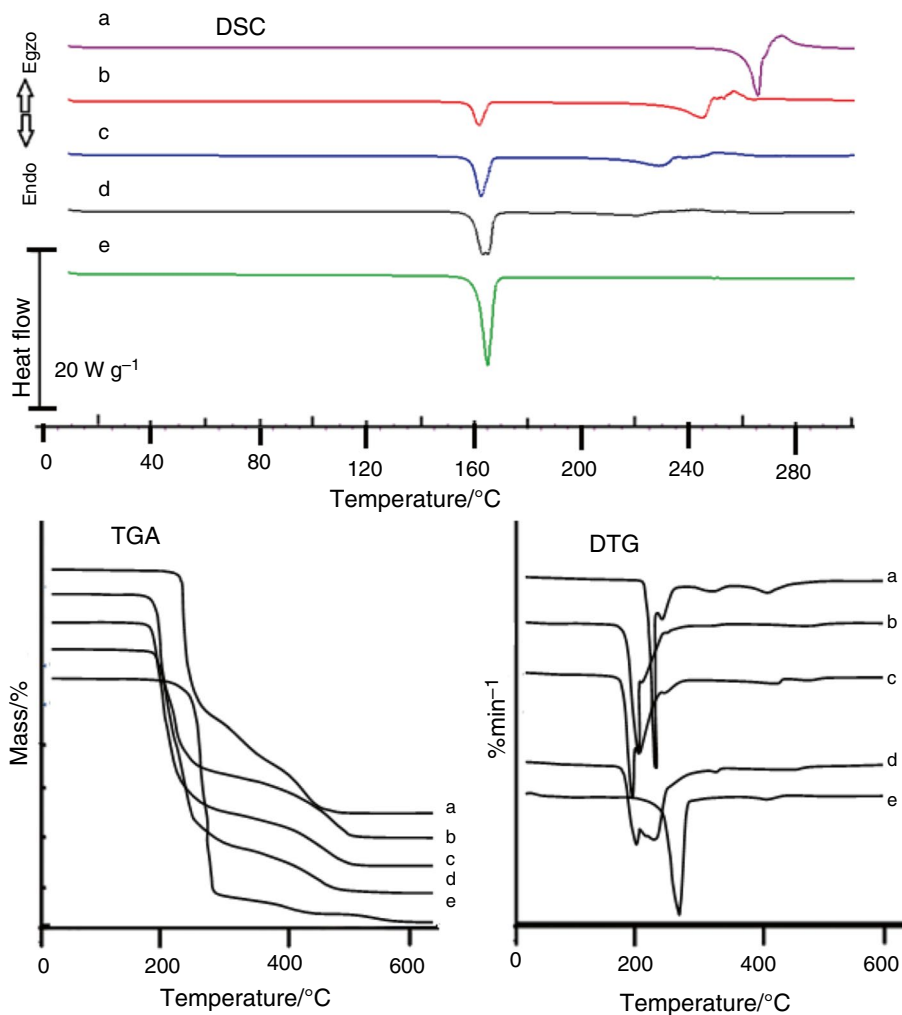
incompatibility with acetylsalicylic acid by lowering its melting point, resulting in the formation of a liquid film on the surface of the magnesium stearate particles which accelerates the decomposition of API. In the case of ibuprofen, incompatibility with stearates leads to the formation of a sublimating eutectic [29]. In turn, β-cyclodextrin, a cyclic oligosaccharide derived from starch, forms inclusion complexes with API [23], due to the structure of β-cyclodextrin, consisting of an outer hydrophilic surface and inner lipophilic cavity. This inclusion complex is formed by the binding of the lipophilic part of the API into the lipophilic cavity of β-cyclodextrin, and the hydrophilic portion of β-cyclodextrin is exposed to the external environment, facilitating the dissolution of API [31]. Thermal data acquired from the DSC and TGA/DTG curves (Tables 1–4) confirm the formation of inclusion complex between acetazolamide and β-cyclodextrin. However, formation of the complex can be called as "non-true incompatibility," because it may improve the properties of the API contributing to its increased solubility.

In contrast, starch is useful as a carrier for amorphous API preparations, as it causes immediate or delayed release of API, and may improve the bioavailability of poorly soluble APIs [23]. Starch is chemically incompatible with ketoconazole, for example, as evidenced by the significantly reduced enthalpy value of their mixture at the ratio 1:1 [32]. PVP has also proved incompatible with a wide range of APIs, despite being used as a binder in tablet preparations, or as a film forming agent and for the formation of amorphous API dispersions [29]. PVP K-30 induces a suppression of the melting point of dexamethasone, which can be explained by the fact that heat assisted dissolution of dexamethasone occurred in the water resulting from PVP dehydration. It may also be feasible that dexamethasone dissolves in the elastic state of the polymer after glazing. Other authors have noted the thermal interactions of PVP with API, in the cases, for example of lipoic acid, diethylcarbamazine citrate and kaempferol [33].

The CA was used to assess the similarities and differences between objects (acetazolamide, excipient and their

Fig. 7 PXRD patterns of **A** a acetazolamide, e chitosan and their mixtures at the ratios: b 7:3, c 1:1 and d 3:7; **B** a acetazolamide, e mannitol and their mixtures at the ratios: b 7:3, c 1:1 and d 3:7
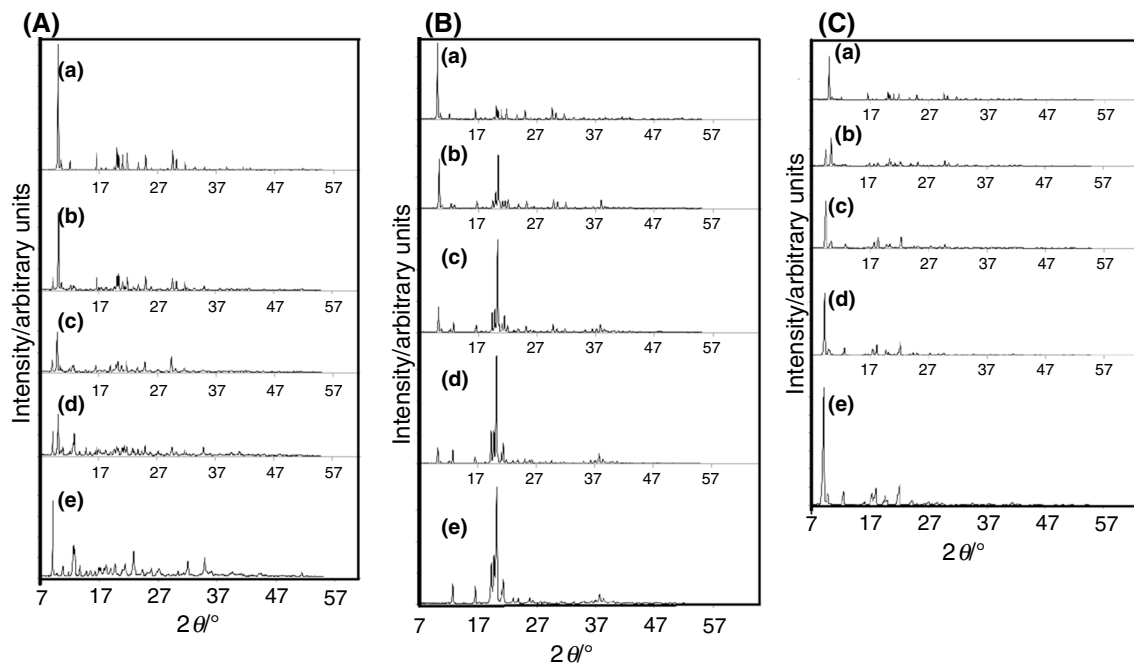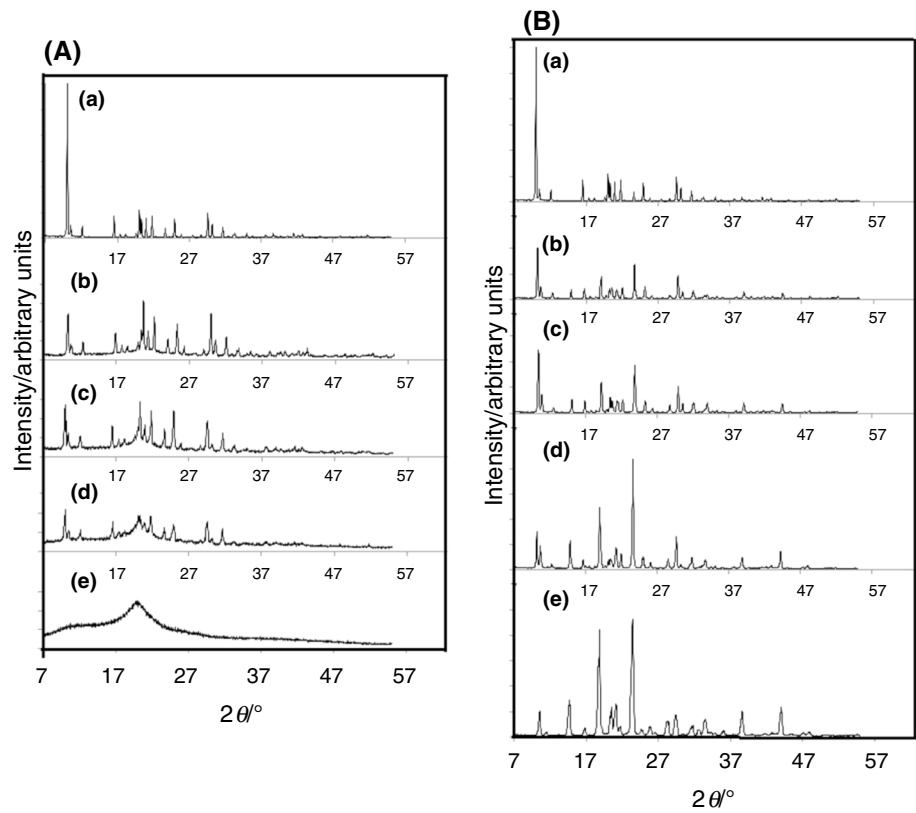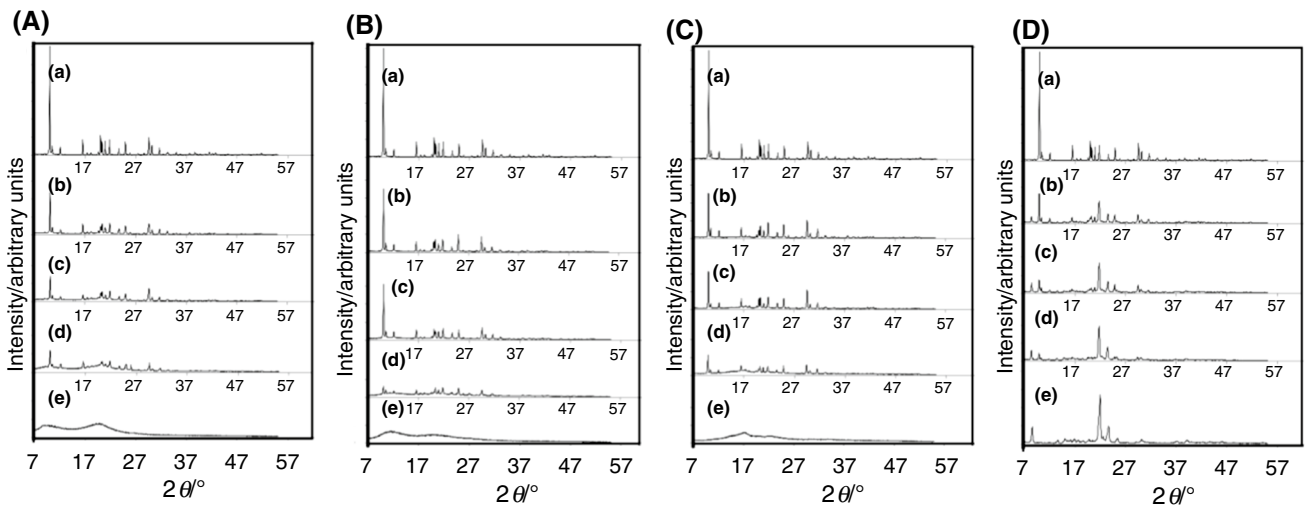

Fig. 8 PXRD patterns of **A** a acetazolamide, e β-cyxclodextrin and their mixtures at the ratios: b 7:3, c 1:1 and d 3:7; **B** a acetazolamide, **e** lactose and their mixtures at the ratios: b 7:3, c 1:1 and d 3:7; **C** a acetazolamide, e meglumine and their mixtures at the ratios: b 7:3, c 1:1 and d 3:7

Fig. 9 PXRD patterns of **A** a acetazolamide, b methylcellulose and their mixtures at the ratios: b 7:3, c 1:1 and d 3:7; **B** a acetazolamide, b PVP K-30 and their mixtures at the ratios: b 7:3, c 1:1 and d 3:7; **C** a acetazolamide, e starch and their mixtures at the ratios: b 7:3, c 1:1 and d 3:7; **D** a acetazolamide, e magnesium stearate and their mixtures at the ratios: b 7:3, c 1:1 and d 3:7
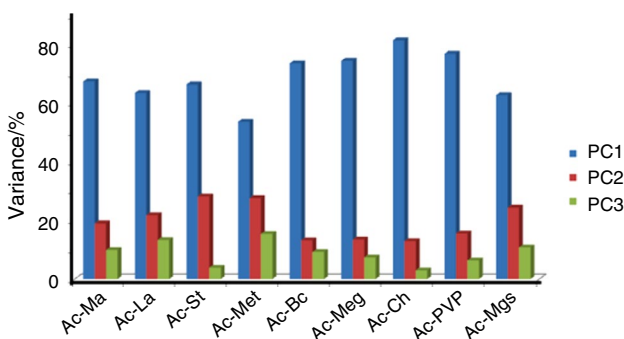

Fig. 10 Variances explained by the first three principal components for acetazolamide mixtures with mannitol (Ac–Ma), lactose (Ac–La), starch 1500 (Ac–St), methylcellulose (Ac–Met), β-cyclodextrin (Ac–Bc), meglumine (Ac–Meg), chitosan (Ac–Ch), PVP K-30 (Ac–PVP) and magnesium stearate (Ac–MgS)

binary mixtures). The crucial point is that objects inside a group should be related to each other but not to objects outside in other groups. Consequently, the greater the similarity within a group, the greater the difference between groups and the more pronounced the clustering [34]. As shown in Fig. 12a, the CA dendrogram for acetazolamide, chitosan and their mixtures revealed four large clusters at 33–66% of the maximum distance. One cluster is formed by chitosan, the second contains two mixtures at ratios of 3:7 and 1:1, the third consists of the 7:3 mixture, and the last includes acetazolamide. This scheme of sample grouping proves the compatibility of ingredients. Conversely, Fig. 12b depicts an example of incompatible ingredients. In this instance, the first cluster contains a 1:1 mixture, the second includes

Fig. 11 PCA score plots for **a** acetazolamide (Ac), chitosan (Ch) and their mixtures at the ratios: 7:3, 1:1 and 3:7; **b** acetazolamide (Ac), mannitol (Ma) and their mixtures at the ratios: 7:3, 1:1 and 3:7
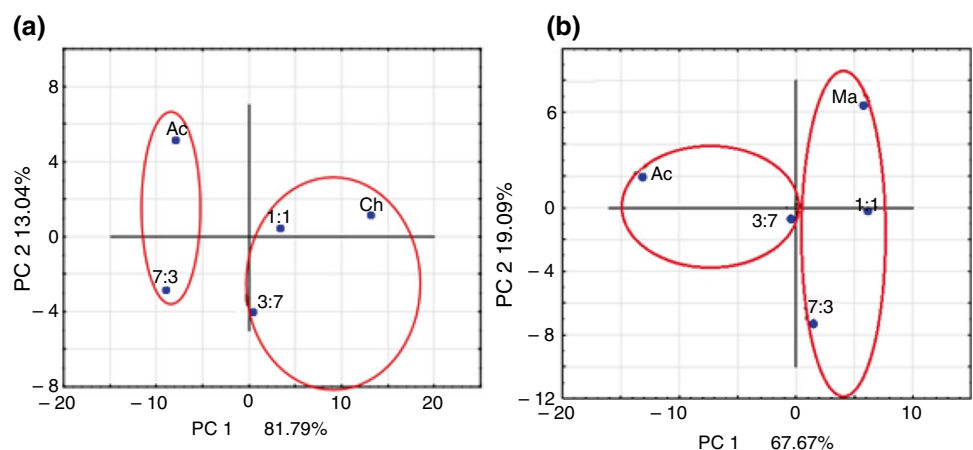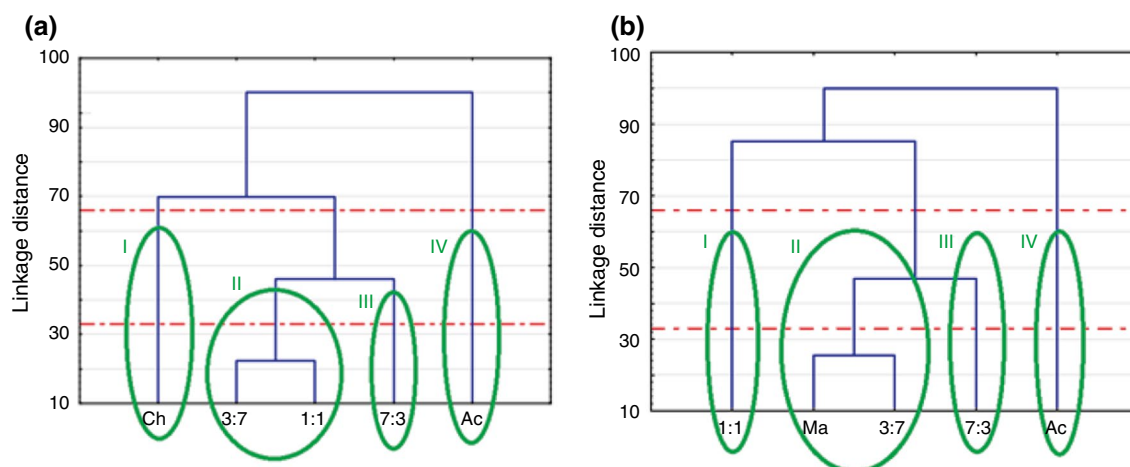
Fig. 12 CA dendrograms for **a** acetazolamide (Ac), chitosan (Ch) and their mixtures at the ratios: 7:3, 1:1 and 3:7; **b** acetazolamide (Ac), mannitol (Ma) and their mixtures at the ratios: 7:3, 1:1 and 3:7

Table 5 Results of the DSC and TGA data interpretation for acetazolamide mixtures with aid of PCA and CA approach

API: excipient	(DSC + TGA) assisted by PCA and CA
Acetazolamide: mannitol	Incompatibility
Acetazolamide: lactose	Incompatibility
Acetazolamide: starch 1500	Incompatibility
Acetazolamide: methylcellulose	Compatibility
Acetazolamide: β-cyclodextrin	Incompatibility
Acetazolamide: meglumine	Incompatibility
Acetazolamide: chitosan	Compatibility
Acetazolamide: PVP K-30	Incompatibility
Acetazolamide: magnesium stearate	Incompatibility

magnesium stearate and 3:7 mixture, while the third consists of a 7:3 mixture, and the fourth contains acetazolamide alone.

Overall, incompatibilities between acetazolamide and mannitol, meglumine, lactose, magnesium stearate, β-cyclodextrin, starch 1500 and PVP K-30 were detected owing to the merging of the DSC and TGA with PCA and CA (Table 5).

Conclusions

The study performed on acetazolamide and its mixtures with selected excipients revealed that the merging of both thermal methods (DSC and TGA) and the additional combination with advanced statistical methods did fulfill their role in predicting incompatibility. PCA was applied to reduce the large thermal data set, with CA being employed to find

similarities between these data. Ultimately, both methods were used to classify the samples. Integrating these methods with the interpretation of DSC and TGA data makes it possible to recognize clearly the presence or absence of incompatibilities. Additional information was also provided by PXRD measurements, which showed that acetazolamide in mixtures did not change its crystalline form at ambient temperature. This indicates that chemical reactions contribute to the incompatibility of acetazolamide with excipients. Finally, DSC along with TGA and supplementary techniques such as PCA and CA ensure reliable results and efficiently confirm the compatibility of API with the excipients under study in acetazolamide mixtures with chitosan and methylcellulose.

References

1. Craig DQM, Reading M. Thermal analysis of pharmaceuticals. Boca Raton: Taylor & Francis Group; 2007.
2. Chadha R, Bhandari S. Drug-excipient compatibility screening. Role of thermoanalytical and spectroscopic techniques. J Pharm Biomed Anal. 2014;87:82–97. https://doi.org/10.1016/j.jpba.2013.06.016.
3. Bejarano A, Nadungodage ChH, Wang F, Catlin ACh, Hoag SW. Decision support for excipient risk assessment in pharmaceutical manufacturing. AAPS PharmSciTech. 2019;20:223. https://doi.org/10.1208/s12249-019-1440-x.
4. Wu Y, Levons J, Narang AS, Raghavan K, Rao VM. Reactive impurities in excipients: profiling, identification and mitigation of drug–excipient incompatibility. AAPS PharmSciTech. 2011;12:1248–63. https://doi.org/10.1208/s12249-011-9677-z.
5. de Lima Gomes EC, de Carvalho IE, Fialho SL, Barbosa J, Yoshida MI, da Silva Cunha Júnior A. Mixing method influence on compatibility and polymorphism studies by DSC and statistical analysis. Application to tenofovir disoproxil fumarate. J Therm Anal Calorim. 2018;131:2123–8. https://doi.org/10.1007/s10973-017-6827-x.
6. Lavor EP, Navarro MVM, Freire FD, Aragão CFS, Raffin FN, Barbosa EG, de Lima e Moura TFA. Application of thermal analysis to the study of antituberculosis drugs-excipient compatibility. J Therm Anal Calorim. 2014;115:2303–9. https://doi.org/10.1007/s10973-013-3050-2.
7. Ali F, Nandi U, Trivedi M, Prakash A, Dahiya M, Lal Sahu P, Kumar R, Nath SG. Quantitative characterization and pharmaceutical compatibility between teneligliptin and widely used excipients by using thermal and liquid chromatography tandem mass spectrometry techniques. J Therm Anal Calorim. 2018;132:385–96. https://doi.org/10.1007/s10973-018-6962-z.
8. Rojek B, Wesolowski M. Thermogravimetric detection of incompatibilities between atenolol and excipients using multivariate techniques. J Therm Anal Calorim. 2013;113:169–77. https://doi.org/10.1007/s10973-013-3070-y.
9. Bannach G, Cervini P, Gomes Cavalheiro ÉT, Ionashiro M. Using thermal and spectroscopic data to investigate the thermal behavior of epinephrine. Thermochim Acta. 2010;499:123–7. https://doi.org/10.1016/j.tca.2009.11.012.
10. Adeyeye MCh, Brittain HG. Preformulation in solid dosage form development. New York: Informa, Healthcare; 2008.
11. Miller JN, Miller JC. Statistics and chemometrics for analytical chemistry. 6th ed. Essex: Pearson Education; 2010.
12. Massart DL, Kaufman L. The interpretation of analytical chemical data by the use of cluster analysis. New York: Wiley; 1983.
13. Schmicki ChN, Owens RL, Orr JE, Edwards BA, Malhotra A. Side effects of acetazolamide: a systematic review and meta-analysis assessing overall risk and dose dependence. BMJ Open Resp Res. 2020;7:e000557. https://doi.org/10.1136/bmjresp-2020-000557.
14. Della Gatta G, Richardson MJ, Sarge SM, Stølen S. Standards, calibration, and guidelines in microcalorimetry. Part 2. Calibration standards for differential scanning calorimetry (IUPAC Technical Report). Pure Appl Chem. 2006;78:1455–76. https://doi.org/10.1351/pac200678071455.
15. Teleginski LK, Maciel AB, Mendes C, Segatto Silva MA, Bernardi LS, de Oliveira PR. Fluconazole–excipient compatibility studies as the first step in the development of a formulation candidate for biowaiver. J Therm Anal Calorim. 2015;120:771–81. https://doi.org/10.1007/s10973-014-4316-z.
16. Roumeli E, Tsiapranta A, Pavlidou E, Vourlias G, Kachrimanis K, Bikiaris D, Chrissafis K. Compatibility study between trandolapril and natural excipients used in solid dosage forms.
17. J Therm Anal Calorim. 2013;111:2109–15. https://doi.org/10.1007/s10973-012-2476-2.
18. Gao R, Jin Y, Yang QY, Sun BW, Lin J. Study of stability and drug-excipient compatibility of estradiol and pharmaceutical excipients. J Therm Anal Calorim. 2015;120:839–45. https://doi.org/10.1007/s10973-014-4234-0.
19. Matos APS, Costa JS, Boniatti J, Seiceira RC, Pitaluga A Jr, Oliveira DL, Viçosa AL, Holandino C. Compatibility study between diazepam and tablet excipients. Infrared spectroscopy and thermal analysis in accelerated stability conditions. J Therm Anal Calorim. 2017;127:1675–82. https://doi.org/10.1007/s10973-016-5350-9.
20. Haynes WM. Handbook of chemistry and physics. 95th ed. Boca Raton 2014-2015: CRC Press LLC; 2014. p. 3–4.
21. Burnham L, Dollimore D, Alexander KS. Kinetic study of the drug acetazolamide using thermogravimetry. Thermochim Acta. 2002;392–393:127–33. https://doi.org/10.1016/S0040-6031(02)00093-X.
22. Rojek B, Wesolowski M. FTIR and TG analyses coupled with factor analysis in a compatibility study of acetazolamide with excipients. Spectrochim Acta Part A. 2019;208:285–93. https://doi.org/10.1016/j.saa.2018.10.020.
23. López FA, Mercê ALR, Alguacil FJ, López-Delgado A. A kinetic study on thermal behavior of chitosan. J Therm Anal Calorim. 2008;91:633–9. https://doi.org/10.1007/s10973-007-8321-3.
24. Rowe RC, Sheskey PJ, Quinn ME. Handbook of pharmaceutical excipients. 6th ed. London: Pharmaceutical Press and American Pharmacists Association; 2009.
25. da Silva EP, Pereira MAV, Lima IPB, Lima NGPB, Barbosa EG, Aragão CFS, Gomes APB. Compatibility study between atorvastatin and excipients using DSC and FTIR. J Therm Anal Calorim. 2016;123:933–9. https://doi.org/10.1007/s10973-015-5077-z.
26. Moraes ANF, Silva LAD, de Oliveira MA, de Oliveira EM, Nascimento TL, Lima EM, Torres LMS, Diniz DGA. Compatibility study of hydroxychloroquine sulfate with pharmaceutical excipients using thermal and nonthermal techniques for the development of hard capsules. J Therm Anal Calorim. 2020;140:2283–92. https://doi.org/10.1007/s10973-019-08953-8.
27. Ladeti I, Bolintineannu S, Vlase G, Cîrcioban D, Ladeti A, Vlase T, Suta LM, Canuii A, Murariu M. Compatibility study between antiparkinsonian drug Levodopa and excipients by FTIR spectroscopy, X-ray diffraction and thermal analysis. J Therm Anal Calorim. 2017;130:433–41. https://doi.org/10.1007/s10973-017-6393-2.
28. Daniel JSP, Cruz JC, Catelani TA, Garcia JS, Trevisan MG. Erythromycin-excipients compatibility studies using the thermal analysis and dynamic thermal infrared spectroscopy coupled with chemometrics. J Therm Anal Calorim. 2021;143:3127–35. https://doi.org/10.1007/s10973-020-09691-y.
29. Bertol CD, Cruz AP, Stulzer HK, Murakami FS, Silva MAS. Thermal decomposition kinetics and compatibility studies of primaquine under isothermal and non-isothermal conditions. J Therm Anal Calorim. 2010;102:187–92. https://doi.org/10.1007/s10973-009-0540-3.
30. Bharate SS, Bharate SB, Bajaj AN. Interactions and incompatibilities of pharmaceutical excipients with active pharmaceutical ingredients: a comprehensive review. J Excip Food Chem. 2010;1:3–26.
31. Li J, Wu Y. Lubricants in pharmaceutical solid dosage forms. Lubricants. 2014;2:21–43. https://doi.org/10.3390/lubricants2010021.
32. Badshah SF, Akhtar N, Minhas MU, Khan KU, Khan S, Abdullah O, Naeem A. Porous and highly responsive cross-linked β-cyclodextrin based nanomatrices for improvement in drug

dissolution and absorption. Life Sci. 2021;267:118931. https://doi.org/10.1016/j.lfs.2020.118931.

32. Lopes MS, Catelani TA, Nascimento ALCS, Garcia JS, Trevisan MG. Ketoconazole: compatibility with pharmaceutical excipients using DSC and TG techniques. J Therm Anal Calorim. 2020;41:1371–8. https://doi.org/10.1007/s10973-019-09137-0.

33. Santos WM, Nóbrega FP, Andrade JC, Almeida LF, Conceição MM, Medeiros ACD, Medeiros FD. Pharmaceutical compatibility of dexamethasone with excipients commonly used in solid dosage forms. J Therm Anal Calorim. 2021;145:361–78. https://doi.org/10.1007/s10973-020-09753-1.

34. Tan PN, Steinbach M, Kumar V. Cluster analysis: basic concepts and algorithms. In: Introduction to data mining. Boston: Addison-Wesley; 2005. p. 487–91.